ELSEVIER

Journal of Power Sources 93 (2001) 77–81

JOURNAL OF POWER SOURCES

www.elsevier.com/locate/jpowsour

Electrode characteristics of nanocrystalline (Zr, Ti)(V, Cr, Ni)$_{2.41}$ compound

W. Majchrzycki[a], M. Jurczyk[b,*]

[a]*Central Laboratory of Batteries and Cells, Forteczna 12/14 St., 61-362 Poznań, Poland*

[b]*Institute of Materials Science and Engineering, Poznań University of Technology, M. Sklodowska Curie 5 Sq., 60-965 Poznań, Poland*

Received 2 March 2000; received in revised form 25 July 2000; accepted 29 July 2000

Abstract

The electrochemical properties of nanocrystalline $Zr_{0.35}Ti_{0.65}V_{0.85}Cr_{0.26}Ni_{1.30}$ alloy, which has the hexagonal C14 type structure, have been investigated. This material has been prepared using mechanical alloying (MA) followed by annealing. The amorphous phase forms directly from the starting mixture of the elements, without other phase formation. Heating the MA samples at 1070 K for 0.5 h resulted in the creation of ordered alloy. This alloy was used as negative electrode for Ni-MH$_x$ battery. The electrochemical results show very little difference between the nanocrystalline and polycrystalline powders, as compared with the substantial difference between these and the amorphous powder. In the annealed nanocrystalline $Zr_{0.35}Ti_{0.65}V_{0.85}Cr_{0.26}Ni_{1.30}$ powders discharging capacities up to 150 mA h g^{-1} (at 160 mA g^{-1} discharging current) have been measured. The properties of nanocrystalline electrode were attributed to the structural characteristics of the compound caused by mechanical alloying.

Keywords: Nanocrystalline; (Zr, Ti)(V, Cr, Ni)$_{2.41}$ alloy; Nickel-metal hydride battery; Electrochemical properties

1. Introduction

There is much interest in Zr-based AB$_2$-type alloys, as many exhibit desirable electrochemical properties, and are among the most promising materials for hydrogen energy applications, such as hydrogen storage materials, heat pumps and electrode materials for rechargeable nickel-metal hydride (Ni-MH$_x$) batteries [1–5]. The ZrV_2 alloy crystallizes in the cubic C15-type structure and at room temperature can absorb up to 5.5 H/f.u. [1]. Nevertheless, the application of these type of materials in batteries has been limited due to poor absorption–desorption kinetics in addition to a complicated activation procedure. Proper engineering of microstructure and surface by using unconventional processing techniques, such as mechanical alloying (MA) [3,6–9] or high-energy ball-milling (HEBM) [10,11], can lead to advanced nanocrystalline intermetallics representing a new generation of metal hydride electrodes. These materials show substantially enhanced absorption characteristics superior to that of the conventionally prepared materials [6]. Recently Zaluski et al. reported also, that powders of nanocrystalline alloys, modified with a catalyst, readily absorb hydrogen, with no need for prior activation [12]. The generation of new metastable phases or materials with an amorphous grain boundary phase offer a wider distribution of available sites for hydrogen and thus a totally different hydrogenation behaviour.

To be useful for storing hydrogen the material should: be capable of storing large quantities of hydrogen; be readily formed and decomposed; have reaction kinetics satisfying the charge–discharge requirements of the system; have the capability of being cycled without alteration in pressure–temperature characteristics during the life of the system; have low hysteresis; have good corrosion stability; have low cost; and be, at least, as safe as other energy carriers.

Recently, it has been shown that the electrochemical properties of ZrV_2-type alloys can be improved by MA [7] or HEBM [11] of the precursor material with a small amount of catalyst powders. On the other hand, the electrochemical activity of these materials can be stimulated by partial substitution in which Zr is partially replaced by Ti, and V is partially replaced by other transition metals (Cr, Mn and Ni) [3,5,13,14]. Some polycrystalline alloys with non-stoichiometric compositions, such as ZrV_{2+x}-type, have also been studied [5].

In this work, the electrochemical properties of nanocrystalline $Zr_{0.35}Ti_{0.65}V_{0.85}Cr_{0.26}Ni_{1.30}$ alloy, which has the hex-

* Corresponding author. Tel.: +48-61-8-351-647; fax: +48-61-665-3576.
E-mail address: jurczyk@sol.put.poznan.pl (M. Jurczyk).

0378-7753/01/$ – see front matter
PII: S0378-7753(00)00565-6

agonal C14 type structure, have been investigated. The mechanically alloyed (Zr, Ti)(V, Cr, Ni)$_{2.41}$ material, in both amorphous and nanocrystalline forms, as well as the conventionally prepared material (pulverized to a fine powder), with 10 wt.% addition of Ni powder, were subjected to electrochemical measurements as working electrodes.

2. Experimental details

2.1. Preparation of the alloys and electrodes

Two different methods were used for preparation the $Zr_{0.35}Ti_{0.65}V_{0.85}Cr_{0.26}Ni_{1.30}$ alloy. Conventionally, the material was prepared by arc melting of stoichiometric amounts of the constituent elements (purity 99.8% or better) in an argon atmosphere. The as cast ingot was homogenized at 1273 K for several days and then rapidly cooled to room temperature in water. The alloy lump was pulverized in a few hydriding–dehydriding cycles to a fine powder ($\leq$45 μm).

In another processing method, mechanical alloying was performed under an argon atmosphere using a SPEX 8000 Mixer Mill. The round-bottom stainless steel vial, which was equipped with a connection valve for evacuation or introduction of argon, was degassed for 12 h below 0.01 Pa. Then high purity argon was introduced into it, the pressure of which was up to 150 kPa. The purity of the starting materials was at least 99.8% and the composition of the starting powder mixture corresponded to the stoichiometry of the ''ideal'' reactions. The elemental powders (Zr: 149 μm; Ti, V: 44 μm; Cr: 1–5 μm and Ni: 3–7 μm) were mixed and poured into the vial. The mill was run up to 30 h for every powder preparation. The as-milled powders were heat treated at 1070 K for 0.5 h under high purity argon to form C14 (hexagonal) phase. The powders were examined by XRD analysis, with Co Kα radiation, at the various stages during milling, prior to annealing and after annealing. The vial was always handled in argon atmosphere to minimize uncontrolled oxidation.

Typical crystallite sizes were estimated from the half-width of lines using the Scherrer equation [15] given by $D_{hkl} = k\lambda/\beta\cos\Theta$, where D_{hkl} is the crystallite size estimated by a (hkl) line, k the Scherrer constant, β the half-width, λ the X-ray wavelength and Θ the diffraction angle. The phases were identified by XRD as well as by scanning electron microscopy (SEM) with an energy-dispersive X-ray microanalysis system (EDS).

The mechanically alloyed (Zr, Ti)(V, Cr, Ni)$_{2.41}$ material, in both amorphous and in nanocrystalline forms, as well as the conventionally prepared material (pulverized to a fine powder), with 10 wt.% addition of Ni powder, were subjected to electrochemical measurements as working electrodes after pressing (under 80 kN cm^{-2}) to 0.5 g pellet form between nickel nets acting as current collector. The diameter of each electrode was 10.4 mm and a thickness of approximately 1.4 mm. Soaking of the electrodes in 12 M KOH solution for 1 h at room temperature with additional etching at 373 K for 10 min in the same solution was sufficient for the initial activation.

2.2. Electrochemical measurements

The electrochemical properties of electrodes were measured in a three-compartment glass cell, using a much larger NiOOH/Ni(OH)$_2$ counter electrode and a Hg/HgO/6 M KOH reference electrode. All electrochemical measurements were carried out in deaerated 6 M KOH solution prepared from Analar grade KOH and 18 M Ω cm^{-1} water, at 293 K. Potentiodynamic and galvanostatic techniques with either short or long-term pulses using a conventional apparatus were applied to study the charge–discharge kinetics of the electrodes. A detailed description of the electrochemical measurements was given in [5].

In the measurements of the electrochemical pressure-composition (e.p.c.) isotherm, after 10 continuous charge–discharge cycles, the electrode was intermittently charged and discharged under galvanostatic conditions with the resting periods (0.5 h) on open circuit long enough for the potential to equilibriate. The capacity obtained during the discharge was used to calculate the amount of hydrogen absorbed on one mole of the electrode material. Hydrogen pressure-composition (p.c.) isotherms for hydrogen absorption–desorption from the gas phase were obtained with a Sievert type apparatus [16].

3. Results and discussion

The behaviour of MA process has been studied by X-ray diffraction, microstructural investigations as well as by electrochemical measurements. Fig. 1 shows a series of XRD spectra of mechanically alloyed Zr-Ti-V-Cr-Ni powder mixture (16.3 wt.% Zr + 15.8 wt.% Ti + 22.1 wt.% V + 6.9 wt.% Cr + 38.9 wt.% Ni) subjected to milling for increasing time. The originally sharp diffraction lines of Zr, Ti, V, Cr and Ni (Fig. 1a) gradually become broader and their intensity decreases with milling time (Fig. 1b). The powder mixture milled for more than 25 h has transformed absolutely to the amorphous phase (Fig. 1c). It is worth noting that before amorphization no shift of the diffraction lines was observed. This result means that the amorphous phase forms directly from the starting mixture of the elements (Zr, Ti, V, Cr and Ni), without formation of other phases. Using the Zr-Ti-V-Cr-Ni mixture composition as the representative material example, the behaviour of the grain size of the crystallites has been studied during the mechanical alloying process. The Ni (1 1 1) diffraction line remains visible up to 15 h of milling. This allows an estimation of the change in the crystalline size of Ni with increase of the milling time. The crystallite size decreases strongly from 50 nm at the beginning of the mechanical alloying process. The final size

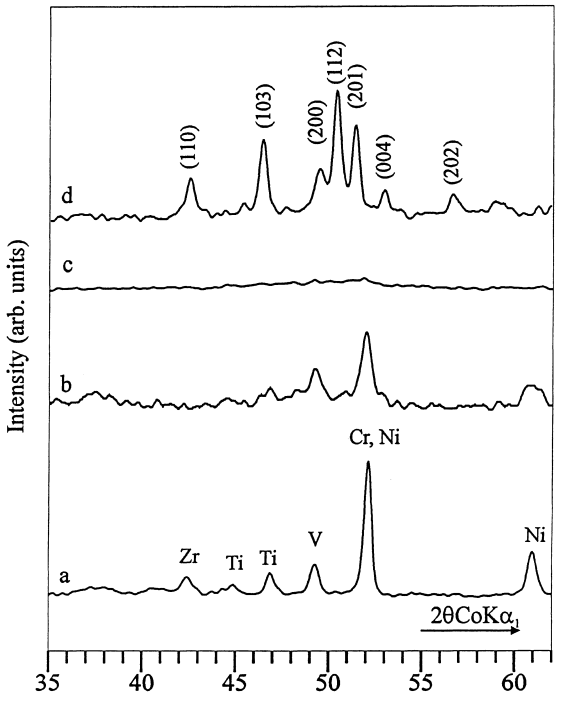

Fig. 1. XRD spectra of a mixture of Zr, Ti, V, Cr and Ni powders mechanically alloyed for different times in an argon atmosphere: (a) initial state (elemental powder mixture); (b) after MA for 5 h; (c) after MA for 25 h and (d) heat treated at 1070 K for 0.5 h.

of the crystallites, about 30 nm, seems to be favourable to the formation of an amorphous phase which develops at the Zr-Ti-V-Cr-Ni interfaces. Formation of alloy with hexagonal C14 type structure was achieved by annealing the amorphous material in high purity argon atmosphere at 1070 K for 0.5 h (Fig. 1d). The final diffraction pattern exhibits broadening of the peaks characteristic of nanocrystalline material. Table 1 reports the cell parameters of the studied materials along with the data obtained for the alloy samples hydrogenated from the gas phase.

The SEM technique was used to follow the changes in size and shape of the mechanically alloyed Zr-Ti-V-Cr-Ni powder mixture as a function of milling time. The microstructure that forms during MA consists of layers of the starting material. The thickness of the material decreases with increase in mechanical alloying time leading to true alloy

Table 1
Structure parameters of $Zr_{0.35}Ti_{0.65}V_{0.85}Cr_{0.26}Ni_{1.30}$ (A) and $Zr_{0.35}Ti_{0.65}V_{0.85}Cr_{0.26}Ni_{1.30}H_x$ (B) prepared by different methods (see text for details)

Preparation method	Composition	a (Å)	c (Å)	V (Å^3)	ΔV (%)
Arc-melting	A	4.935	8.030	169	–
	B	5.098	8.753	197	17
Mechanical alloying and annealing	A	4.921	8.011	168	–
	B	5.092	8.684	195	16

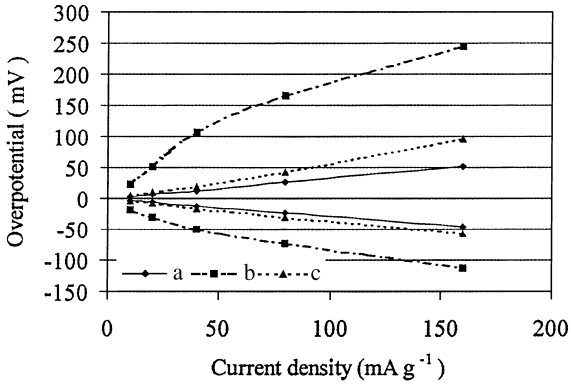

Fig. 2. Overpotential against current density on activated: (a) polycrystalline; (b) amorphous and (c) nanocrystalline $Zr_{0.35}Ti_{0.65}V_{0.85}Cr_{0.26}Ni_{1.30}$ electrodes, at 15 s of anodic and cathodic galvanostatic pulses.

formation [7]. The sample shows cleavage fracture morphology and inhomogeneous size distribution.

To study the quality of the activated polycrystalline, amorphous and nanocrystalline $Zr_{0.35}Ti_{0.65}V_{0.85}Cr_{0.26}Ni_{1.30}$, as electrode materials in the Ni-MH_x battery, the overpotential against current density was recorded at 15 s of anodic and cathodic galvanostatic pulses (Fig. 2). It can be seen that the anodic and cathodic parts of polycrystalline and nanocrystalline electrodes are almost symmetrical with respect to the rest potential of electrode. It may be concluded that for both electrodes fast discharge rates can be achieved.

The electrochemical pressure-composition (e.p.c.) isotherms for absorption and desorption of hydrogen were obtained from the equilibrium potential values of the electrodes, measured during intermittent charge and/or discharge cycles at constant current density, by using the Nernst equation according to the procedure reported by Balej [17]. The e.p.c. isotherms determined on the studied materials are illustrated in Fig. 3. Due to the amorphous nature of the $Zr_{0.35}Ti_{0.65}V_{0.85}Cr_{0.26}Ni_{1.30}$ alloy prior to annealing (curve (b) on Fig. 3), the hydrogen absorption–desorption characteristics are not satisfactory. Annealing causes transformation from the amorphous to the crystalline

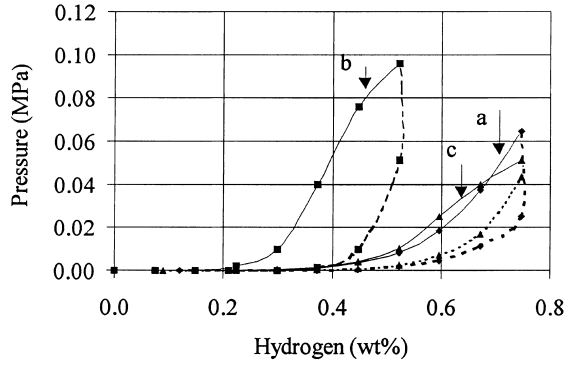

Fig. 3. Electrochemical pressure-composition isotherm for absorption (solid line) and desorption (dashed line) of hydrogen on: (a) polycrystalline; (b) amorphous and (c) nanocrystalline $Zr_{0.35}Ti_{0.65}V_{0.85}Cr_{0.26}Ni_{1.30}$, at 293 K.

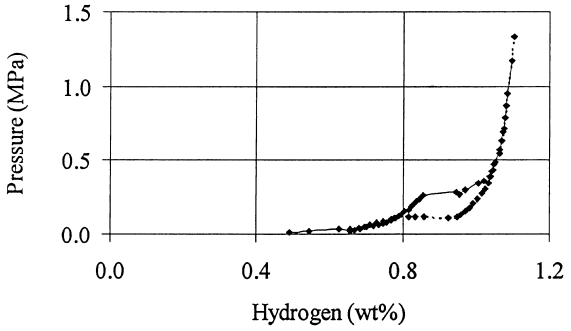

Fig. 4. Pressure composition isotherm for absorption (solid line) and desorption (dashed line) of hydrogen from the gas phase on polycrystalline $Zr_{0.35}Ti_{0.65}V_{0.85}Cr_{0.26}Ni_{1.30}$, at 293 K.

structure and produces grain boundaries. Anani et al. [3] noted that grain boundaries are necessary for the migration of the hydrogen into the alloy. It is worth noting from Fig. 3 that the characteristics for polycrystalline and nanocrystalline materials are very similar in respect to hydrogen contents, but there are small differences in the plateau pressures.

For comparison, Fig. 4 shows the storage capacity of polycrystalline $Zr_{0.35}Ti_{0.65}V_{0.85}Cr_{0.26}Ni_{1.30}$ alloy for hydrogen absorption and desorption from the gas phase, as characterized by equilibrium hydrogen pressure against hydrogen content isotherms (p.c.) measured using Sievert equipment. From Figs. 3 and 4 it is apparent that at similar pressure (0.06 MPa) the chemical and electrochemical uptakes of hydrogen are about equal (~0.7 wt.%). The much greater chemical uptake of hydrogen is at much higher, up to 1.3 MPa.

The typical galvanostatic discharge curves of the electrodes fabricated from the polycrystalline, amorphous and nanocrystalline $Zr_{0.35}Ti_{0.65}V_{0.85}Cr_{0.26}Ni_{1.30}$ materials are shown in Fig. 5. It can be seen, the discharge capacities of polycrystalline as well nanocrystalline electrodes are almost the same. As shown in this Figure, the galvanostatic discharge characteristics of the Ni-MH_x battery with an amorphous material as the negative electrode is clearly lower.

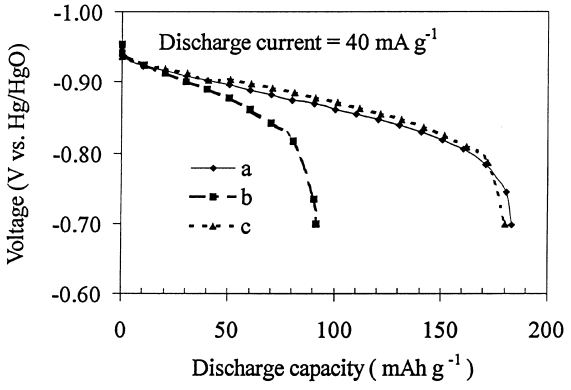

Fig. 5. Discharge curves of (a) polycrystalline; (b) amorphous and (c) nanocrystalline $Zr_{0.35}Ti_{0.65}V_{0.85}Cr_{0.26}Ni_{1.30}$ electrodes, at seventh cycle (current density of 40 mA g^{-1} in 6 M KOH).

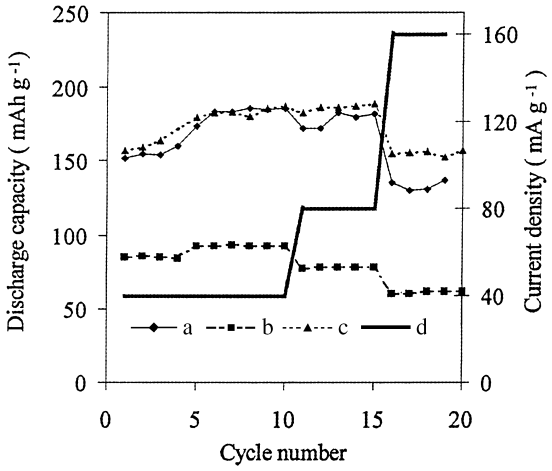

Fig. 6. Discharge capacity as a function of cycle numbers of electrode prepared with (a) polycrystalline; (b) amorphous and (c) nanocrystalline $Zr_{0.35}Ti_{0.65}V_{0.85}Cr_{0.26}Ni_{1.30}$ (solution: 6M KOH; temperature: 293 K). The charge conditions were: 40 mA g^{-1}; the discharge conditions were plotted in (d); cut-off potential vs. Hg/HgO/6 M KOH was of −0.7 V.

Table 2
Discharge capacities of $Zr_{0.35}Ti_{0.65}V_{0.85}Cr_{0.26}Ni_{1.30}$ material prepared by arc melting and mechanical alloying and annealing (current density of charging and discharging was 160 mA g^{-1})

Preparation method	Structure type	Discharge capacity at 18 cycle (mA h g^{-1})
Arc-melting	Polycrystalline ($MgZn_2$)	135
Mechanical alloying	Amorphous	65
Mechanical alloying and annealing	Nanocrystalline ($MgZn_2$)	145

Fig. 6 shows the discharge capacities of the electrodes as a function of charge–discharge cycling number. The electrode prepared with nanocrystalline $Zr_{0.35}Ti_{0.65}V_{0.85}Cr_{0.26}Ni_{1.30}$ material showed better activation and higher discharge capacities. This improvement is due to a well-established diffusion path for hydrogen atoms along the numerous grain boundaries [18]. It is worth noting, that annealed nanocrystalline powder has greater capacities than the amorphous parent alloy powders. Table 2 reports the discharge capacities of the studied materials. In our earlier work, it was confirmed that the discharge capacity of electrodes prepared by application of MA ZrV_2 alloy powder with 10 wt.% of Ni powder addition could not be estimated because of extremely high polarization [7]. Materials obtained when Ti was substituted for Zr and Cr, Ni was substituted for V in ZrV_2 lead to greatly improved activation behaviour of the electrodes.

4. Conclusion

In conclusion, nanocrystalline $Zr_{0.35}Ti_{0.65}V_{0.85}Cr_{0.26}Ni_{1.30}$ alloy synthesized by mechanical alloying was used

as negative electrode materials for Ni-MH_x battery. The amorphous phase forms directly from the starting mixture of the elements, without other phase formation. Heating the MA samples at 1070 K for 0.5 h resulted in the creation of ordered ZrV_2-type alloy. The electrochemical results show very little difference between the nanocrystalline and polycrystalline powders, as compared with the substantial difference between these and the amorphous powder. In the annealed nanocrystalline $Zr_{0.35}Ti_{0.65}V_{0.85}Cr_{0.26}Ni_{1.30}$ powder discharging capacities up to 150 mA h g^{-1} (at 160 mA g^{-1} discharge current) have been measured. The properties of nanocrystalline electrode were attributed to the structural characteristics of the compound caused by mechanical alloying.

Acknowledgements

The financial support of the Polish National Committee for Scientific Research (KBN) under the contract No. 7 T08D 015 12 is gratefully acknowledged.

References

[1] K.H.J. Buschow, P.C.P. Bouten, A.R. Miedema, Rep. Prog. Phys. 45 (1982) 937.
[2] G. Sandrock, S. Suda, L. Schlapbach, Hydrogen in intermetallic compounds II, in: L. Schlapbach (Ed.), Topics in Applied Physics, Vol. 67, Springer, Berlin, 1992 (Chapter 5).
[3] A. Anani, A. Visintin, K. Petrov, S. Srinivasan, J.J. Reilly, J.R. Johnson, R.B. Schwarz, P.B. Desch, J. Power Sources 47 (1994) 261.
[4] T. Sakai, M. Matsuoka, C. Iwakura, in: K.A. Gschneider Jr., L. Eyring (Eds.), Handbook on the Physics and Chemistry of Rare Earth, Vol. 21, Elsevier, Amsterdam, 1995, p. 135.
[5] M. Kopczyk, G. Wojcik, G. Mlynarek, A. Sierczynska, M. Beltowska-Brzezinska, J. Appl. Electrochem. 26 (1996) 639.
[6] L. Zaluski, A. Zaluska, J.O. Ström-Olsen, J. Alloys Comp. 217 (1995) 245.
[7] M. Jurczyk, W. Rajewski, G. Wojcik, W. Majchrzycki, J. Alloys Comp. 285 (1999) 250.
[8] Z. Chen, Z. Chen, Y. Su, M. Lü, D. Zhou, P. Huang, Mater. Res. Bull. 33 (1998) 1449.
[9] M. Jurczyk, W. Rajewski, W. Majchrzycki, G. Wojcik, J. Alloys Comp. 290 (1999) 262.
[10] M. Au, F. Pourarian, S. Simizu, S.G. Sankar, L. Zhang, J. Alloys Comp. 223 (1995) 1.
[11] M. Jurczyk, W. Rajewski, W. Majchrzycki, G. Wojcik, J. Alloys Comp. 274 (1998) 299.
[12] L. Zaluski, A. Zaluska, J.O. Ström-Olsen, J. Alloys Comp. 253–254 (1997) 70.
[13] H. Nakano, S. Wakao, J. Alloys Comp. 231 (1995) 587.
[14] F.-J. Liu, S. Suda, J. Alloys Comp. 231 (1995) 666.
[15] B.D. Cullity, Elements of X-ray Diffraction, Addison-Wesley, Reading, MA, 1978.
[16] A. Sievert, A. Gatta, Z. Anorg. Chem. 172 (1928) 1.
[17] J. Balej, Int. J. Hydrogen Energy 10 (1985) 363.
[18] P. Selvam, B. Viswanathan, J. Less-Common Met. 163 (1990) 89.